Zero Reaction Maneuver: Flight Validation with ETS-VII Space Robot and Extension to Kinematically Redundant Arm

Kazuya Yoshida, Kenichi Hashizume and **Satoko Abiko**

Department of Aeronautics and Space Engineering, Tohoku University,
Aoba 01, Sendai 980-8579, JAPAN,
yoshida@astro.mech.tohoku.ac.jp

Abstract

This paper presents the experimental results and post-flight analysis of Reaction Null-Space based reactionless manipulation, or Zero Reaction Maneuver (ZRM). The concept has been developed with an insight into the motion dynamics of free-flying multi-body systems and its practical availability is clearly demonstrated with ETS-VII, a Japanese space robot. The ZRM is proven particularly useful to remove the velocity limit of manipulation due to the reaction constraint and the time loss due to the waiting for the attitude recovery. The existence of the ZRM is very limited for a 6 DOF manipulator arm mounted on a free-flying base, but it is discussed that more operational freedom is obtained with a kinematically redundant arm.

1. Introduction

The Engineering Test Satellite VII (ETS-VII), Figure 1, developed and launched by National Space Development Agency of Japan (NASDA) has been successfully flown and carried out a lot of interesting orbital robotics experiments with a 2 meter-long, 6 DOF manipulator arm mounted on this un-manned spacecraft.

The ideas for the rescue or service to a malfunctioning satellite by a free-flying space robot has been discussed since early 80s (for example [1]), but very few attempts have ever done in orbit. The maintenance missions of the Hubble Space Telescope and the retrieval of the Space Flyer Unit are such important examples carried out with the Space Shuttle Remote Manipulator System. However, in these missions the manipulator was manually operated by a well-trained flight crew. Autonomous target capture by an un-manned space robot is a big challenge for space robotics community for many years, and very recently, essential parts of this technology have been successfully verified and demonstrated in orbit by ETS-VII.

The mission objective of ETS-VII is to test robotics technology and demonstrate its utility for un-manned orbital operation and servicing tasks. The mission consists of two subtasks, autonomous rendezvous/docking (RVD) and robot experiments (RBT). The robot experiments include a variety of topics such as: (1) teleoperation from the ground with large time-delay, (2) robotic servicing task demonstrations such as ORU exchange and deployment of a space structure, (3) dynamically coordinated control between the manipulator reaction and the satellite attitude, and (4) capture and berthing of a target satellite. Early reports on some of these experiments were made in [2][3][7][9], for example.

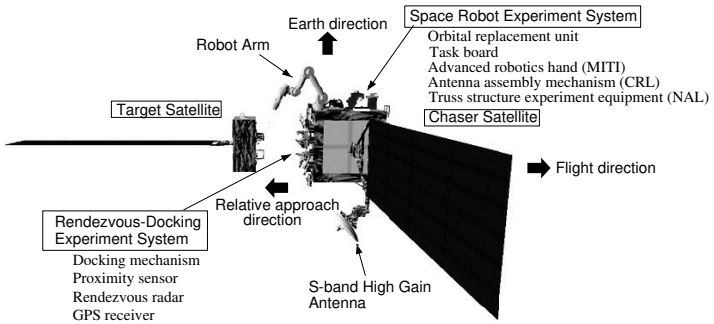

Figure 1: The Engineering Test Satellite VII

The initially planned flight experiments were successfully completed by the end of May 1999. But since the ETS-VII was still operational in a good condition, an extensive mission period was set till the end of December 1999. In this period the opportunity was opened for academic proposals and four research groups from Japanese universities were given the time to do their own flight experiments. The groups and their topics are (A) Tohoku University 1: several different dynamic control methods, which is elaborated in this paper, (B) Tohoku University 2: teleoperation using a 6DOF haptic interface device, (C) Tokyo Institute of Technology: identification of the vibratory dynamics, and (D) Kyoto University: teleoperation with a bilateral force feedback control.

The present authors carefully prepared for the above flight experiments (A) and have successfully

obtained invaluable flight data, where the focus was made on the dynamic characteristics of the base/arm coupling and coordination. Specific research subjects and corresponding flight data have been reported in [8]:

(a) manipulation in the inertial space using the Generalized Jacobian Matrix,

(b) reactionless manipulations based on the Reaction Null-Space,

(c) non-holonomic path planning and operation for terminal endpoint control,

(d) coordinated control between the manipulator arm and the base satellite by feedback control with offset attitude commands.

Above all, the results of the reactionless manipulation, or *Zero Reaction Maneuver,* are so clear and obvious that the attitude of the base satellite has kept very close to zero while the manipulator arm makes motion from a given point to another with following the reactionless path obtained from the Reaction Null-Space theory. The Zero Reaction Maneuver should be very useful for future space operations, because one of the reasons why the current manipulator motion in space is so slowly is due to the restriction on the base reaction, and this restriction would be removed.

This paper focuses on the background theory, flight data analysis, and further discussion for more practical usage of the Zero Reaction Maneuver by a manipulator arm with more DOF.

The paper is organized as follows. In Section 2, the formulation of dynamics, particularly about the Reaction Null-Space is briefly reviewed. In Section 3, the flight data of the extended ETS-VII flight experiments are presented, and Section 4 extends the discussion to the case with a redundant arm.

2. Dynamics and Control of a Free-Flying Space Robot

A unique characteristics of a free-flying space robot is found in its motion dynamics. According to the motion of the manipulator arm, the base spacecraft moves due to the action-to-reaction principle or the momentum conservation. The reaction of the arm disturbs its footing base, then the coupling and coordination between the arm and the base becomes an important issue for successful operation. This is a main difference from a terrestrially based robot manipulator and a drawback to make the control of a space manipulator difficult. Earlier studies for the modeling and control of such a free-flying robot are collected in the book [4].

2.1. Basic equations

The equation of motion of a free-flying space robot as a multibody system is, in general, expressed in the following form:

$$\begin{bmatrix} \boldsymbol{H}_b & \boldsymbol{H}_{bm} \\ \boldsymbol{H}_{bm}^T & \boldsymbol{H}_m \end{bmatrix} \begin{bmatrix} \ddot{\boldsymbol{x}}_b \\ \ddot{\boldsymbol{\phi}} \end{bmatrix} + \begin{bmatrix} \boldsymbol{c}_b \\ \boldsymbol{c}_m \end{bmatrix} = \begin{bmatrix} \mathcal{F}_b \\ \boldsymbol{\tau} \end{bmatrix} + \begin{bmatrix} \boldsymbol{J}_b^T \\ \boldsymbol{J}_m^T \end{bmatrix} \mathcal{F}_h \quad (1)$$

where we choose the linear and angular velocity of the base satellite (reference body) $\dot{\boldsymbol{x}}_b = (\boldsymbol{v}_b^T, \boldsymbol{\omega}_b^T)^T$ and the motion rate of the manipulator joints $\dot{\boldsymbol{\phi}}$ as generalized coordinates. The formulation is not limited to a single, serial-link manipulator arm, but in this paper, we suppose one serial manipulator system with n Degrees-Of-Freedom (DOF) is mounted on a base body. The symbols used here are defined as follows:

$\boldsymbol{H}_b \in R^{6\times 6}$: inertia matrix of the base.

$\boldsymbol{H}_m \in R^{n\times n}$: inertia matrix for the manipulator arms (the links except the base.)

$\boldsymbol{H}_{bm} \in R^{6\times n}$: coupling inertia matrix.

$\boldsymbol{c}_b \in R^6$: velocity dependent non-linear term for the base.

$\boldsymbol{c}_m \in R^6$: that for the manipulator arms.

$\mathcal{F}_b \in R^6$: force and moment exert on the centroid of the base.

$\mathcal{F}_h \in R^6$: those exert on the manipulator hand.

$\boldsymbol{\tau} \in R^n$: torque on the manipulator joints.

Especially in the free-*floating* situation, the external force/moment on the base, which can be generated by gas-jet thrusters, and those on the manipulator hand are assumed zero; i.e. $\mathcal{F}_b = \boldsymbol{0}$, $\mathcal{F}_h = \boldsymbol{0}$. The motion of the robot is governed by only internal torque on the manipulator joints $\boldsymbol{\tau}$, and hence the linear and angular momenta of the system $(\mathcal{P}^T, \mathcal{L}^T)^T$ remain constant.

$$\begin{bmatrix} \mathcal{P} \\ \mathcal{L} \end{bmatrix} = \boldsymbol{H}_b \dot{\boldsymbol{x}}_b + \boldsymbol{H}_{bm} \dot{\boldsymbol{\phi}} \quad (2)$$

2.2. Angular momentum

The integral of the upper set of the equation (1) gives the momentum conservation, as shown in Equation (2), which is composed of the linear and angular momenta. The linear momentum has further integral to yield the principle that the mass centroid stays stationary or linearly moves with a constant velocity.

The angular momentum equation, however, does not have the second-order integral hence provides the first-order non-holonomic constraint. The equation is

expressed in the form with the angular velocity of the base $\boldsymbol{\omega}_b$ and the motion rate of the manipulator arm $\dot{\boldsymbol{\phi}}$ as:

$$\tilde{\boldsymbol{H}}_b\boldsymbol{\omega}_b + \tilde{\boldsymbol{H}}_{bm}\dot{\boldsymbol{\phi}} = \mathcal{L} \tag{3}$$

where $\mathcal{L}$ is the initial constant of the angular momentum, and the inertia matrices with a tilde are those modified from Equation (2). $\tilde{\boldsymbol{H}}_{bm}\dot{\boldsymbol{\phi}}$ represents the angular momentum generated by the manipulator motion.

2.3. Manipulation with zero disturbance to the base

From a practical point of view, the attitude change is not desirable, then the manipulator motion planning methods to have minimum attitude disturbance on the base are also well studied. An ultimate goal of those approaches is completely zero disturbance, and such operation is found with an insight into the angular momentum equation.

The angular momentum equation with zero initial constant $\mathcal{L} = \boldsymbol{0}$ and zero attitude disturbance $\boldsymbol{\omega}_b = \boldsymbol{0}$:

$$\tilde{\boldsymbol{H}}_{bm}\dot{\boldsymbol{\phi}} = \boldsymbol{0} \tag{4}$$

yields the following null-space solution:

$$\dot{\boldsymbol{\phi}} = (\boldsymbol{I} - \tilde{\boldsymbol{H}}_{bm}^{+}\tilde{\boldsymbol{H}}_{bm})\dot{\boldsymbol{\zeta}} \tag{5}$$

The joint motion given by this equation is guaranteed to make zero disturbance on the base attitude. Here the vector $\dot{\boldsymbol{\zeta}}$ is arbitrary and the null-space of the inertia matrix $\tilde{\boldsymbol{H}}_{bm}$ is termed *Reaction Null-Space* (RNS) [5].

The rank of this null-space projector is $n-3$, while for the ETS-VII the manipulator arm has 6 DOF, i.e. $n = 6$, then there remains 3 DOF for additional criterion to specify $\dot{\boldsymbol{\zeta}}$.

By the way, the manipulator hand motion observed in the satellite base frame $\dot{\boldsymbol{x}}_h = (\boldsymbol{v}_h^T, \boldsymbol{\omega}_h^T)^T$ are expressed as:

$$\begin{bmatrix} \boldsymbol{v}_h \\ \boldsymbol{\omega}_h \end{bmatrix} = \begin{bmatrix} \boldsymbol{J}_v \\ \boldsymbol{J}_\omega \end{bmatrix} \dot{\boldsymbol{\phi}} \tag{6}$$

using conventional Jacobian matrices.

If paying attention to either upper set or lower set of Equation (6), each of them has 3 DOF, then can be a good candidate for this motion constraint.

Let us consider to combine Equations (4) and the lower set of (6):

$$\begin{bmatrix} \tilde{\boldsymbol{H}}_{bm} \\ \boldsymbol{J}_\omega \end{bmatrix} \dot{\boldsymbol{\phi}} = \begin{bmatrix} \boldsymbol{0} \\ \boldsymbol{\omega}_h \end{bmatrix} \tag{7}$$

The solution for $\dot{\boldsymbol{\phi}}$ gives the manipulator motion to generate zero reaction on the base, while the orientation change of the hand, $\boldsymbol{\omega}_h$, is specified or constraint.

In case of the ETS-VII, where the combined inertia and Jacobian matrix

$$\boldsymbol{G} = \begin{bmatrix} \tilde{\boldsymbol{H}}_{bm} \\ \boldsymbol{J}_\omega \end{bmatrix} \tag{8}$$

is a 6 by 6 square matrix. Its solution is then obtained with a matrix inversion as follows, as far as the matrix is not singular.

$$\dot{\boldsymbol{\phi}} = \begin{bmatrix} \tilde{\boldsymbol{H}}_{bm} \\ \boldsymbol{J}_\omega \end{bmatrix}^{-1} \begin{bmatrix} \boldsymbol{0} \\ \boldsymbol{\omega}_h \end{bmatrix} \tag{9}$$

This solution belongs to the Reaction Null-Space given by Equation (5), but unique since any freedom is not left over due to the kinematic constraint introduced in (7).

Note again that the manipulator motion given by this unique solution yields both zero reaction on the base and the specified orientation change of the hand. However, any specification or constraint has not been made on the translational motion of the hand: eventually it moves and the motion trace forms a line. This *resultant* motion of the hand is calculated by plugging Equation (9) into the upper set of (6).

$$\boldsymbol{v}_h = \boldsymbol{J}_v\boldsymbol{G}^{-1} \begin{bmatrix} \boldsymbol{0} \\ \boldsymbol{\omega}_h \end{bmatrix} \tag{10}$$

Again, $\boldsymbol{v}_h$ is a unique solution.

For the Zero Reaction Maneuver tested on the ETS-VII, we prepared several motion paths from or to a given point in the operational space. The motion trace is obtained by a numerical integration of Equation (10) with a constant, non-zero $\boldsymbol{\omega}_h$. As both $\boldsymbol{v}_h$ and $\boldsymbol{\omega}_h$ are dependent in a complex way, several different $\boldsymbol{\omega}_h$ are tried and the resultant $\boldsymbol{v}_h$ are checked in advance simulation, then a most suitable operation is picked up for the flight experiment.

2.4. Singularity Consistent Inversion

In the above process, the operation to obtain $\boldsymbol{v}_h$ includes the inversion of $\boldsymbol{G}$. Unlike conventional Jacobians or inertia matrices, the combined matrix $\boldsymbol{G}$ may involve many singular points in a non-intuitive manner. And at or around a singular point, the inversion is not defined or yields unstable solution.

In order to obtain stable solutions near the singularity, a good computational method using the following equation is developed [6]:

$$\dot{\boldsymbol{\phi}} = k \cdot \mathrm{adj}(\boldsymbol{G})\dot{\boldsymbol{x}} \tag{11}$$

where k is an arbitrary scaler and $\dot{\boldsymbol{x}}$ stands for $(\boldsymbol{0}, \boldsymbol{\omega}_h^T)^T$. If k is chosen as $k = 1/\det(\boldsymbol{G})$, then the computation becomes same as with the conventional inverse, and a finite k works to bound the magnitude of $\dot{\boldsymbol{\phi}}$ in the vicinity of the singularity.

We employed this method in the practical computation.

3. Flight Experiments

The extended flight experiment proposed by Tohoku University was carried out on September 30, 1999, using three successive *flight paths*. The flight path is a

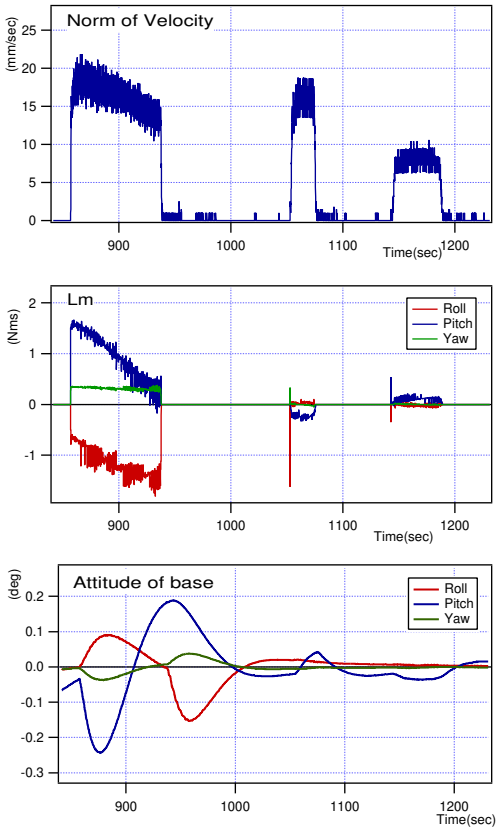

Figure 2: ETS-VII flight data for the RNS based reactionless manipulation

communication window between Tsukuba Space Center, NASDA, and ETS-VII via TDRS, a US data relay satellite located in GEO above the pacific ocean. In each flight path almost net 20 minutes operation (command uplink) and dense telemetry (including video downlink) are allowed.

For our experiments, the manipulator motion trajectories were carefully prepared in a motion file and the safety was preliminary checked on an offline simulator. During the experiment, the motion file is uploaded to ETS-VII at 4 Hz frequency as an isochronous command and the manipulator arm in space is controlled to follow these given trajectories.

In this paper, the focus is made on the experimental result of the RNS based reactionless manipulation only.

3.1. RNS based reactionless manipulation

In the RNS experiment, several sets of reactionless trajectories were prepared using Equation (10) with (11). We prepare the trajectories to go to or from a useful control point such as a standard approach point (150 [mm] right above the corresponding optical marker) to an onboard ORU or a target satellite, and compared with the motion by conventional PTP trajectories.

The experiment was carried out under the attitude control of the base satellite using reaction wheels. Even under the control, the attitude disturbance is observed when the base receives the manipulator reaction, since the control torque of reaction wheels is relatively small. The attitude control here mainly works for the recovery after the attitude disturbed.

Figure 2 depicts a typical flight data to compare the conventional and reactionless manipulations. The top graph shows the velocity norm of the manipulator hand. The middle shows the reaction momentum induced by the manipulation. And the bottom shows the attitude motion. The graphs include three sets of manipulator motion, the first one is the conventional PTP manipulation generating a relatively large momentum and attitude disturbance, while the other two are the RNS based reactionless manipulation yielding very small, almost zero reaction and disturbance.

It should be noted that, not only the maximum attitude change is remarkably different, but the time for the recovery is also very different. This waiting time for the attitude recovery in the conventional manipulation is not negligible and degrade the efficiency of the operation in practice. However, the reactionless manipulation, or Zero Raction Maneuver, provides almost zero attitude disturbance and almost zero recovery time, thus assures a very high operational efficiency.

4. Extension to the Case with a Redundant Manipulator Arm

The flight experiments have been carried out under the practical constraints of an existing flight system, ETS-VII. Of particular since ETS-VII has a 6 DOF manipulator arm, non-redundant in trivial sense, the trajectories for Zero Reaction Maneuver are too much constraint to perform Point-To-Point operation from a given initial point A to an arbitrary goal point B. In this section, we discuss how this characteristics could change if we would have a 7 or more DOF manipulator arm.

Let us recall Equations (9) and (10). When $n = 6$ these equations represents a fully determined system, and the integration of (10) yields a one-dimensional line in the operational space.

Now let us consider the cases with $n > 6$. In these cases, the matrix $\boldsymbol{G}$ becomes non-square, $6 \times n$, then a general solution for $\dot{\boldsymbol{\phi}}$ is given with a pseudo inverse component and a null-space component:

$$\dot{\boldsymbol{\phi}} = \boldsymbol{G}^{\#} \begin{bmatrix} \boldsymbol{0} \\ \boldsymbol{\omega}_h \end{bmatrix} + (\boldsymbol{I} - \boldsymbol{G}^{\#}\boldsymbol{G})\dot{\boldsymbol{\xi}} \qquad (12)$$

$$\boldsymbol{v}_h = \boldsymbol{J}_v \boldsymbol{G}^{\#} \begin{bmatrix} \boldsymbol{0} \\ \boldsymbol{\omega}_h \end{bmatrix} + \boldsymbol{J}_v(\boldsymbol{I} - \boldsymbol{G}^{\#}\boldsymbol{G})\dot{\boldsymbol{\xi}} \qquad (13)$$

In case of $n = 7$, the solution for $\dot{\boldsymbol{\phi}}$ stays on a plane in the configuration space given by mutually perpendicular two vectors, the first term and the second term

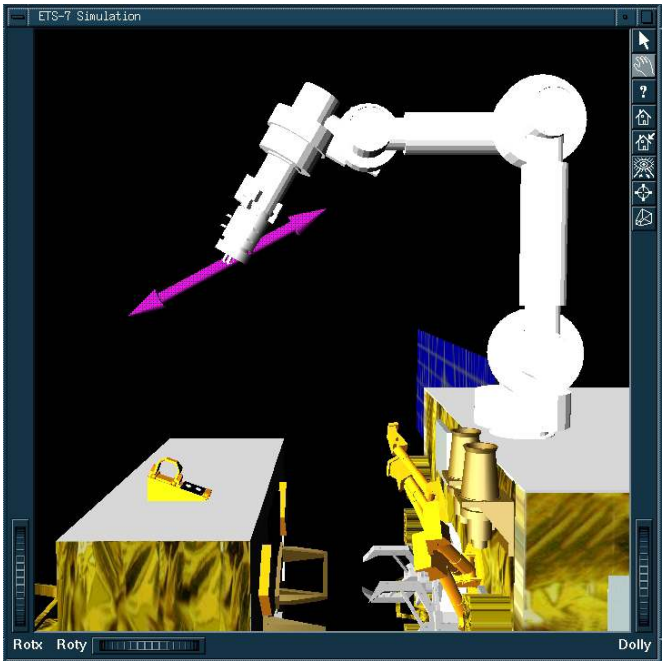

Figure 3: A direction for a reactionless path when $n = 6$

of (12). And the solution for $\boldsymbol{v}_h$ stays on a plane in the operational space given by two vectors, the first term and the second term of (13).

Note that in both spaces, the second term vector has variable magnitude according to the variety of $\dot{\boldsymbol{\xi}}$ but its direction is all the same, invariant for a given configuration. Also in the operational space, the two vectors are not necessary perpendicular but the summation of two stays on a plane which includes both vectors.

Practical situations are compared with computer graphic images. Figure 3 depicts a case with a 6 DOF manipulator arm. For an arbitrary input of $\boldsymbol{\omega}_h$ there exists a single instantaneous direction for the hand to move while keeping zero attitude change for the base and the given motion for the hand orientation. Figure 4 depicts a case with a 7 DOF manipulator arm. In this case, there are choices of the instantaneous motion direction of the hand from a plane illustrated here, for an arbitrary input of $\boldsymbol{\omega}_h$. The size of the lateral component depends on $\dot{\boldsymbol{\xi}}$ of Equation (13).

Figure 5 illustrates an application to a motion planning toward a specified terminal point, such as a fixture mounted on a free-floating target satellite. In case with a 6 DOF manipulator arm we cannot expect that a terminal point always stays on a reactionless path [10], but as illustrated here, Zero Reaction Maneuver with some operational flexibility would be possible with a 7 DOF manipulator arm.

However, it should be note that there still remains constraint and some degrees of difficulty in the operation. We need $\boldsymbol{\omega}_h$ as a driving input, and we may need non-holonomic planning to locate the hand with

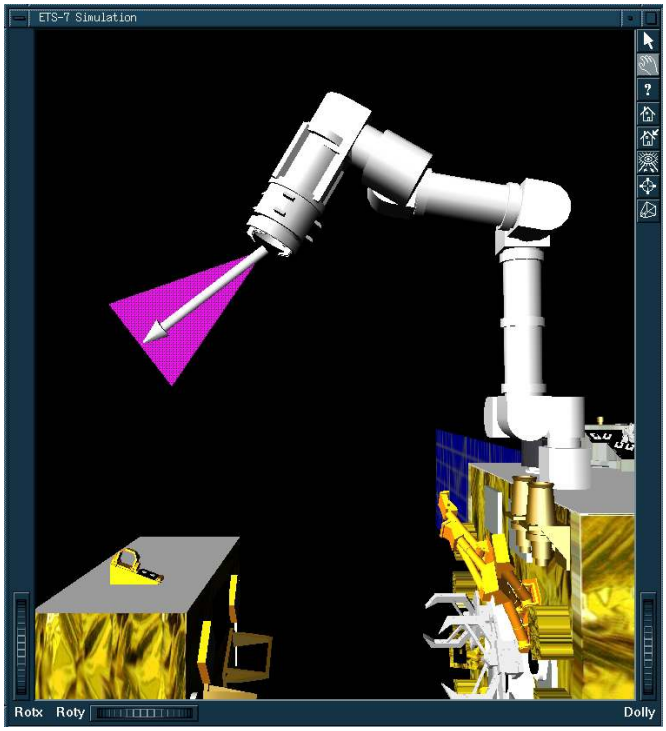

Figure 4: A plane for reactionless paths when $n = 7$

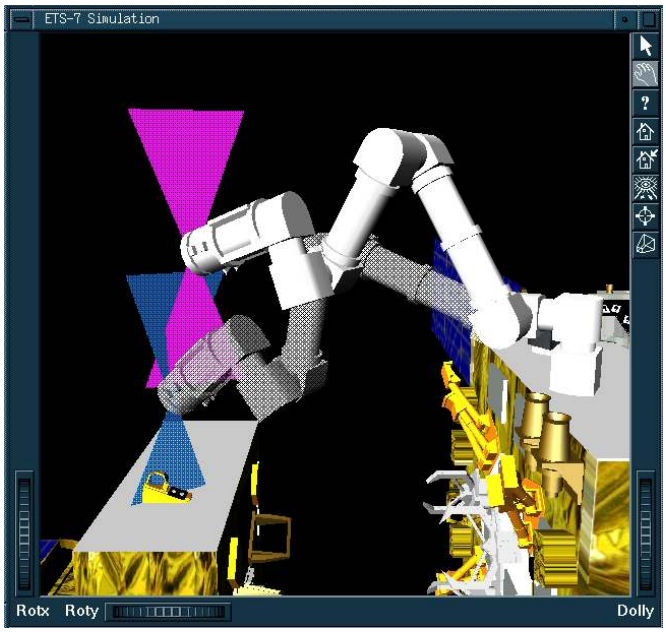

Figure 5: Example of the motion planning to a given goal with Zero Reaction Maneuver ($n = 7$)

a proper orientation, which is left for further investigation.

It is inferred that the possible directions of the hand motion would form a three-dimensional space when the arm has 8 DOF. And the Zero Reaction Maneuver without any operational constraint, except singularities, would be possible with a 9 DOF arm.

5. Conclusions

This paper summarizes the experimental results and post-flight analysis of Reaction Null-Space based reactionless manipulation, or Zero Reaction Maneuver. This concept has been developed with an insight into the motion dynamics of free-flying multibody systems and its practical availability is demonstrated by the extended flight experiments carried out in September 1999 on ETS-VII, a Japanese space robot.

It is clearly verified with the Zero Reaction Maneuver that the attitude disturbance of the base is kept almost zero during manipulator tasks, and it is particularly useful to remove the velocity limit of manipulation due to the reaction constraint and the time loss due to the waiting for the attitude recovery.

Such Zero Reaction Maneuvers (ZRM) are very specified for a 6 DOF manipulator arm mounted on a free-flying base, but it is clarified that more operational freedom is obtained with a kinematically redundant arm. An instantaneous ZRM direction forms a specific vector with a 6 DOF arm, but is can be chosen from a plane with a 7 DOF arm and from a 3-D space with a 8 DOF arm. Fully arbitrary ZRM, in the sense that zero attitude change of the base, can be achieved with a 9 DOF arm.

References

[1] D. L. Akin, M. L. Minsky, E. D. Thiel and C. R. Curtzman, "Space Applications of Automation, Robotics and Machine Intelligence Systems (ARAMIS) phase II," *NASA-CR-3734 – 3736,* 1983.

[2] M. Oda et al, "ETS-VII, Space Robot In-Orbit Experiment Satellite," *Proc. 1996 IEEE Int. Conf. on Robotics and Automation,* pp.739–744, 1996.

[3] There are a number of papers reporting the ETS-VII flight experiments in *Proc. 5th Int. Symp. on AI, Robotics and Automation in Space, i-SAIRAS'99,* June 1999, ESTEC, Netherlands.

[4] *Space Robotics: Dynamics and Control,* edited by Xu and Kanade, Kluwer Academic Publishers, 1993.

[5] K. Yoshida, D. N. Nenchev and M. Uchiyama, "Moving base robotics and reaction management control," *Robotics Research: The Seventh International Symposium*, Ed. by G. Giralt and G. Hirzinger, Springer Verlag, 1996, pp. 101–109.

[6] Y. Tsumaki, D. N. Nenchev and M. Uchiyama, "Jacobian Adjoint Matrix Based Approach to Teleoperation," *Proc. Int. Symp. of Microsystems, Intelligent Materials and Robots,* Sendai, Japan, pp.532-535, 1995.

[7] N. Inaba and M. Oda, "Autonomous Satellite Capture by a Space Robot," *Proc. 2000 IEEE Int. Conf. on Robotics and Automation,* pp.1169–1174, 2000.

[8] K. Yoshida, D. N. Nenchev, N. Inaba and M. Oda, "Extended ETS-VII Experiments for Space Robot Dynamics and Attitude Disturbance Control," *22nd Int. Symp. on Space Technology and Science,* ISTS2000-d-29, Morioka, Japan, May, 2000.

[9] K. Yoshida, K. Hashizume, D. N. Nenchev, N. Inaba and M. Oda, "Control of a Space Manipulator for Autonamous Target Capture –ETS-VII Flight Experiments and Analysis–," *AIAA Guidance, Navigation, and Control Conference & Exhibit,* AIAA2000-4376, Denver, CO, August, 2000.

[10] D. N. Nenchev and K. Yoshida, "Point-To-Point and Reactionless Motions of a Free-Flying Space Robot," *Proc. 2001 IEEE Int. Conf. on Robotics and Automation,* submitted.